Limnol. Oceanogr., 59(6), 2014, 2185–2202

doi:10.4319/lo.2014.59.6.2185

Prediction of surface temperature in lakes with different morphology using air temperature

Marco Toffolon,[1]* Sebastiano Piccolroaz,[1] Bruno Majone,[1] Anna-Maria Soja,[2] Frank Peeters,[3] Martin Schmid,[4] and Alfred Wüest [4,5]

[1] Department of Civil, Environmental and Mechanical Engineering, University of Trento, Italy
[2] Health & Environment Department, AIT Austrian Institute of Technology GmbH, Tulln, Austria
[3] Limnological Institute, University of Konstanz, Konstanz, Germany
[4] Eawag, Swiss Federal Institute of Aquatic Science and Technology, Surface Waters—Research and Management, Kastanienbaum, Switzerland
[5] Physics of Aquatic Systems Laboratory—Margaretha Kamprad Chair, École Polytechnique Fédérale de Lausanne—School of Architecture, Civil and Environmental Engineering—Environmental Engineering Institute, Lausanne, Switzerland

Abstract

Temperature of the surface layer of temperate lakes is reconstructed by means of a simplified model on the basis of air temperature alone. The comparison between calculated and observed data shows a remarkable agreement (Nash–Sutcliffe efficiency indices always larger than 0.87, mean absolute errors of approximately 1°C) for all 14 lakes investigated (Mara, Sparkling, Superior, Michigan, Huron, Erie, Ontario, Biel, Zurich, Constance, Garda, Neusiedl, Balaton, and Baikal, in west-to-east order), which present a wide range of morphological and hydrological characteristics. Differently from a pure heat flux balance approach, where the different fluxes are determined on the basis of independent relationships, the input data directly inform parameters of a simple model that, in turn, provides meaningful information about the properties of the real system. The dependence of the model parameters on the main morphological indicators is presented, which allows for a quantitative description of the strong influence of the mean depth of the lake on the thermal inertia and the hysteresis pattern between air and lake surface temperatures.

The temperature of the surface layer is a crucial factor for the hydrodynamics and ecology of lakes. Water temperature changes may have important direct and indirect ecological effects via their influence on the life-history processes of organisms (metabolism, growth, reproduction) and the properties of the habitats (Winder and Sommer 2012). Temperature variations affect food-web structures and the availability of nutrients for the biological systems in a lake. The effects of temperature on physical and chemical characteristics of lakes may also modify the distribution of individual taxa from the microbiological to the top predator scale (Eggermont and Heiri 2012; Wojtal-Frankiewicz 2012; De Senerpont Domis et al. 2013).

Surface temperature is the result of heat fluxes at the lake surface (short-wave solar radiation, long-wave radiation from and to the lake, sensible and latent heat exchange) and at the boundaries (inflows and outflows, groundwater exchange, precipitation, etc.), and of heat transport due to mixing within the lake. All these fluxes depend on several variables (solar radiation, air temperature, wind speed and direction, cloudiness, relative humidity, etc.), some of which may be difficult or expensive to measure reliably and with sufficient precision. Moreover, some of the variables can change significantly over the lake surface and in time (e.g., wind), and reconstructing their spatial variation can be a particularly hard task. Predicting water temperature is nonetheless a desired goal and models of different types and of different complexity have been proposed, ranging from simple regression models (Livingstone and Lotter 1998; Sharma et al. 2008) to more complex process-based numerical one-dimensional (Goudsmit et al. 2002; Perroud et al. 2009; Thiery et al. 2014) and three-dimensional models (Wahl and Peeters 2014).

In this work, we aim at obtaining results that are accurate enough to reliably predict the annual cycle of lake surface temperature and its interannual variability, using a simple model that requires a minimum amount of information. In particular, we assume that air temperature is a proxy for the integrated effect of the relevant processes and fluxes (Livingstone and Padisák 2007) and that can be used as the unique input variable of the model. A similar assumption has been introduced also in studies concerning other environments, like rivers, estuaries, and bays (Morrill et al. 2005; Cho and Lee 2012).

We apply a simple lumped model (Piccolroaz et al. 2013) that has been developed to estimate water temperature in the well-mixed surface layer (approximately corresponding to the epilimnion) as a function of air temperature only to several different lakes. The model is based on physical considerations, but it is elaborated in the simple form of an ordinary differential equation that contains a small number of parameters (from four to eight in different versions). These parameters summarize the role of several processes in the heat budget, and are calibrated solely with records of air and water temperature data, ideally covering a sufficiently long time window to capture full interannual variability. The fact that the model is data driven, while

* Corresponding author: marco.toffolon@unitn.it

being based on physical grounds, allows for the direct acquisition of information about the studied system. The variable role of the different heat fluxes is implicitly reconstructed by the calibration of the parameters, which hence assume a descriptive character that can be used to classify the thermal behavior of each lake.

Various classifications of lakes have been proposed in the past (Hutchinson and Löffler 1956; Lewis 1983; *see* also Boehrer and Schultze 2008, for a review on stratification patterns) that are generally formulated in qualitative terms or are mainly descriptive. Here we show that the thermal dynamics can vary significantly with the morphological features. In particular, the average depth plays a crucial role in the response of the lake surface temperature to air temperature: e.g., shallow lakes usually react more rapidly to the seasonal change of the atmospheric conditions compared with large and deep lakes. Although this may seem an obvious consideration, the identification of the main parameters affecting the thermal response of lakes is not trivial and represents the only possibility to attain prediction capabilities. This is especially important in ungauged lakes.

In the following sections, we briefly describe the model and the lakes used as case studies. Then we analyze the performance of the model in reproducing lake surface temperature dynamics and present the dependence of the parameters on the main hydromorphological quantities. Finally, we interpret the role of the parameters in the light of a simplified analytical solution and discuss the implications of the results for a thermal characterization of lakes.

Methods

Formulation of the model—We are interested in exploiting a simplified model to determine medium- and long-term variations (from seasonal to decadal) of surface temperatures in natural lakes when a limited amount of measured data is available. To this aim, we adopt the air2water model that has been recently proposed by Piccolroaz et al. (2013) and that relies on air temperature as the only external meteorological forcing.

In general, the surface heat budget affects only a portion of the whole lake volume. Referring to this layer, the heat balance can be presented in the following form:

$$V_s \frac{dT_w}{dt} = A \frac{\Phi_{net}}{\rho c_p} \tag{1}$$

where t is time, ρ is the water density, c_p is its specific heat, V_s is the volume of the surface layer for which the temperature T_w is representative, A is the surface area of the lake, and Φ_{net} is the net heat flux per unit surface through the lake surface area. The heat flux exchange with the deep water or the sediments is not explicitly considered, but the calibration of the model parameters can implicitly account for this contribution (Piccolroaz et al. 2013). By defining the average depth of the surface layer $D_s = V_s A^{-1}$, Eq. 1 can be rewritten as:

$$\frac{dT_w}{dt} = \frac{\Phi_{net}}{\rho c_p D_s} = \frac{1}{\delta} \frac{\Phi_{net}}{\rho c_p D_r} \tag{2}$$

where we introduce $\delta = V_s V_r^{-1}$ as the ratio between the volume of the surface layer, V_s, and a reference volume, V_r. δ can also be interpreted as the ratio between the average depth of the surface layer D_s and the average reference depth $D_r = V_r A^{-1}$. Equation 2 suggests that the rate of change of lake surface temperature is inversely proportional to the mean depth of the volume affected by the heat exchange. It is worth noticing that V_s typically varies in time due to its dependence on the thermal stratification of the water column, which plays a crucial role in the heating process. The right-hand side of Eq. 2 represents the effective contribution of the heat fluxes to the lake surface temperature dynamics, and can be expressed as the sum of several components (short- and long-wave radiation, sensible and latent fluxes, inflows and outflows, etc.). Therefore, estimating the net heat flux requires the precise consideration of all contributing fluxes. For this purpose, process-based models are generally used, which allow for an accurate description of the independent processes. However, this kind of model requires a large amount of information (e.g., wind forcing, air temperature, net solar radiation, humidity, cloudiness) that is not always easy to gather, especially over long time periods.

The model air2water is based on a simplification of the heat budget (Eq. 1) in which it is assumed that T_a can be considered as the main factor driving the change of T_w. In particular, with reference to temperate lakes, the model assumes that T_a is a proxy for almost all the relevant processes affecting the net heat flux (Piccolroaz et al. 2013). In this way, after suitable simplifications, Eq. 2 can be rewritten in the form of an ordinary differential equation depending on a reduced number of parameters. Here we present the model in two different formulations, considering four and eight parameters, respectively.

In this work, we reformulate the eight-parameter version of the model in the following equivalent form:

$$\frac{dT_w}{dt} = \frac{1}{\delta}\left\{a_1 + a_2 T_a - a_3 T_w + a_5 \cos\left[2\pi\left(\frac{t}{t_y} - a_6\right)\right]\right\} \tag{3}$$

where t_y is the duration of a year in the adopted units, which reflects the assumption that the sum of the external forcing can be described with a sinusoidal term characterized by a primary annual period, and a_1 to a_6 are model parameters. In the model, δ is estimated as a function of the difference of surface temperature and the temperature T_h of the hypolimnion (4°C for dimictic lakes, and the minimum or maximum water temperature for warm and cold monomictic lakes, respectively):

$$\begin{aligned} \delta &= \exp\left(-\frac{T_w - T_h}{a_4}\right) && \text{for} \quad T_w \geq T_h \\ \delta &= \exp\left(-\frac{T_h - T_w}{a_7}\right) + \exp\left(-\frac{T_w}{a_8}\right) && \text{for} \quad T_w < T_h \end{aligned} \tag{4}$$

The volume ratio δ is theoretically defined in the range between 0 and 1, with the value 1 corresponding to the maximum volume of the surface layer, and decreasing values accounting for increasingly strong stratification, which reduce the water volume affected by the surface heat budget.

We note that Eq. 3 is slightly different from the corresponding original equation presented in Piccolroaz et al. (2013), while maintaining the same mathematical meaning: the parameter a_1 corresponds to p_3 in that paper, a_2 to p_4, a_3 to p_4-p_5, a_4 to p_6, a_5 to p_1, a_6 to p_2, a_7 to p_7, and a_8 to p_8. The physical meaning of the parameters can be summarized as follows: Parameters a_5 and a_6 describe the amplitude and the phase of the overall annual external meteorological forcing term, parameters a_2 and a_3 account for the processes that depend on air temperature and lake surface temperature, respectively, and indirectly on the difference $T_a - T_w$, whereas a_1 includes the residual effect. The parameter a_4 corresponds to the scale of lake surface temperature that determines the strength of the thermal stratification (for temperatures warmer than T_h). The parameter a_7 has the same meaning but it is used to reproduce the inverse stratification for temperatures lower than T_h, and the parameter a_8 accounts for the effect of heat flux reduction during the ice-covered period by means of a fictitious increase of the effective volume δ. Moreover, a lower bound is imposed on lake surface temperature by introducing a threshold value that is assumed to represent ice formation on the surface. This threshold is generally 0°C when the water temperature is measured close to the surface, but it can be higher for those cases where temperature is measured at higher depths (e.g., Lake Baikal; *see* also next section).

The second version that we consider here is the simplest one, the four-parameter model, which does not include the externally imposed sinusoidal forcing,

$$\frac{dT_w}{dt} = \frac{1}{\delta}\{a_1 + a_2 T_a - a_3 T_w\} \tag{5}$$

and is based on the assumption that the volume ratio does not vary for temperatures lower than T_h:

$$\begin{cases} \delta = \exp\left(-\dfrac{T_w - T_h}{a_4}\right) & \text{for} \quad T_w \geq T_h \\ \delta = 1 & \text{for} \quad T_w < T_h \end{cases} \tag{6}$$

In this case the physical meaning of the parameters differs from the case of the eight-parameter version, and the terms including T_a and T_w, which both have an annual periodicity, indirectly take into account the periodicity of external meteorological forcing. These assumptions allow for a more strict identification of the parameter values as will be discussed later.

Both versions of the model are reminiscent of the physics of the phenomena, but the mathematical formulation is in general highly simplified, so that it is not possible to choose the values of the parameters in a deterministic way. However, reasonable ranges can be defined for the parameters on the basis of physical considerations, so they can be effectively calibrated using long-term records of measured air and lake surface temperatures. Given the simplicity of the model, a Monte Carlo calibration procedure can be performed using a large number of randomly chosen sets of parameters (10^8 realizations in the examined cases). The objective function during the calibration is the Nash–Sutcliffe efficiency index E (Nash and Sutcliffe 1970): a value $E = 1$ corresponds to a perfect match between measured and simulated values, whereas $E = 0$ indicates that the model prediction is as accurate as the mean of observations (negative values would indicate that the mean of observations is a better estimator than the model itself). The calibration has been performed in two steps: first, a wide range of the parameter values was explored; then, a narrower range was selected around the sets giving the highest values of E to find the best simulation with a higher degree of accuracy.

It is important to note that the models given by Eqs. 3 and 5 are characterized by a very general structure; thus the calibration of the parameters is the essential element of the procedure by which the model is informed by the measurements. As a whole, the model is able to respond to variable climatic conditions, suggesting that, despite the simple formulation, the most important processes are included.

Morphological characterization of the selected lakes and data availability—In the present study we consider 14 lakes. Following the west-to-east order indicated in Fig. 1: Lake Mara (a southern arm of Lake Shuswap, in Canada), Lake Sparkling (a small lake in northern Wisconsin), Lake Superior, Lake Michigan, Lake Huron, Lake Erie, and Lake Ontario (Great Lakes at the border between U.S.A. and Canada), Lake Biel and Lake Zurich (Switzerland), Lake Constance (at the border of Germany, Switzerland, and Austria), Lake Garda (northern Italy), Lake Neusiedl (a very shallow lake at the border between Austria and Hungary), Lake Balaton (a very shallow lake in Hungary), and Lake Baikal (the deepest and most voluminous lake on Earth, located in Siberia, Russia). All these lakes are temperate and are located in a relatively narrow range of latitudes, but they significantly differ with respect to morphological features and mixing regimes, thus representing an interesting data set for the presented analysis.

In Table 1 we present the main geometrical quantities characterizing these lakes: volume V, surface area A, maximum depth H, mean depth $D = VA^{-1}$, equivalent diameter of a circle having the same surface as the lake $L = 2\sqrt{A\,\pi^{-1}}$, relative depth HL^{-1} (Wetzel and Likens 1991). We also include the hydraulic residence time $t_r = VQ^{-1}$, where Q is the reference value of the outflow estimated from available data sets. Supplementary information is presented in Fig. 2 for a visual overview of the extreme differences among the lakes' geometrical characteristics. Apart from an obvious growing trend of the volume with the surface, we can see that there are no obvious relationships for the other parameters. For instance, the relative depth HL^{-1} is independent from the area and some of the lakes appear to be relatively shallow despite being deep in absolute terms (e.g., Superior, Michigan, Ontario, Huron). The residence time is quite variable too, and very small lakes like Sparkling can have a very long t_r comparable with much larger lakes. As a whole, the extreme variability of the characteristics of the examined lakes represents a challenge for a simple model.

The data sets of air and lake surface temperatures for the selected lakes were not uniform. For some of them long

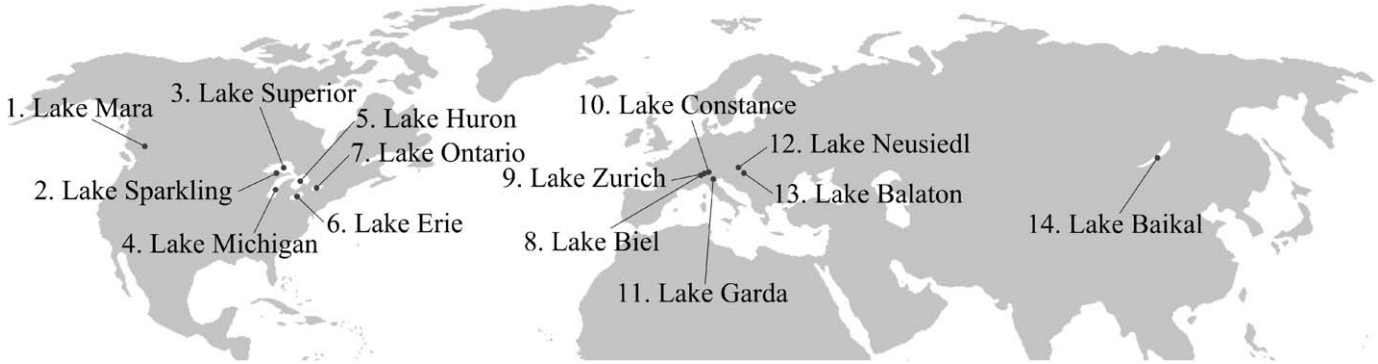

Fig. 1. Approximate geographical locations of the selected lakes.

records could be used (e.g., daily time series of 27 yr for Lakes Superior, Michigan, and Erie, and 36 yr for Lake Neusiedl), whereas for other cases only short, discontinuous series or series with low temporal resolution (e.g., single measurements with monthly frequency) were available. Moreover, for some lakes we considered both in situ measurements (buoy or shoreline stations) and temperature reconstruction on the basis of satellite imagery. The data sets are described in Table 2.

We applied the model air2water in the eight-parameter and four-parameter versions to the selected lakes, with a daily computational time step. For those cases for which long historical time series of daily air and lake surface temperatures were available, the calibration of the parameters was performed using two-thirds of the data set and leaving one-third for the validation, whereas in the other cases the whole record was used for model calibration and no validation was performed (Table 2). When only monthly lake surface temperature measurements were available, the model was applied with a daily time step, and the Nash–Sutcliffe efficiency index E was evaluated using those single monthly values (if the date of the measurement was known) or monthly averages (if the available data were averages or no information was available about the date of measurement). Given the limited amount of information, in these cases the entire data set was used for model calibration, with the exception of Lake Balaton, which boasts a 49 yr long historical record. Finally, for the case of Lake Baikal, since the data of air and lake surface temperatures available for the analysis overlap only for 2 yr (Table 2), the calibration has been performed by referring to the mean annual cycles of air and lake surface temperatures.

Results

Application of the model—For all the lakes examined, a satisfactory reproduction of both seasonal and interannual fluctuations of lake surface temperature has been achieved, as demonstrated by the high values of E reported in Table 3 for the eight-parameter model and in Table 4 for the four-parameter model. The root mean-square errors (RMSEs) and the absolute mean errors are relatively small as well, and comparable with those obtained by using process-based models (Stefan et al. 1998; Peeters et al. 2002; Thiery et al. 2014), which, however, require a complete set of meteorological data as input, whereas our formulation needs air temperature only. As an example, we report a direct comparison of model performances with the SimStrat model (Goudsmit et al. 2002), which has been adopted by Peeters et al. (2002) for the interpretation of long-term historical data of lake surface temperatures in Lake Zurich. The RMSE at the lake surface reported by the authors is 0.77°C for SimStrat, to be compared with 0.92°C for air2water (*see* Table 4).

Table 1. Morphological characteristics of the selected lakes.

No.	Lake	A (km^2)	V (km^3)	H (m)	D (m)	L (km)	HL^{-1} (10^{-3})	t_r (yr)
1	Mara	19	0.35	46	18	5	9.4	2
2	Sparkling	0.64	0.0088	20	14	1	22.2	10
3	Superior	82,100	12,000	406	146	323	1.3	191
4	Michigan	58,000	4900	281	84	272	1.0	99
5	Huron	59,600	3543	229	59	275	0.8	22
6	Erie	25,667	480	64	19	181	0.4	2.6
7	Ontario	19,000	1640	244	86	156	1.6	6
8	Biel	39.3	1.2	74	30	7	10.5	0.2
9	Zurich	67.3	3.3	136	49	9	15.4	1.2
10	Constance	536	48	254	90	26	9.7	4.3
11	Garda	370	50	346	135	22	15.9	26.8
12	Neusiedl	315	0.325	1.8	1	20	0.1	1.5
13	Balaton	593	1.9	12.2	3	27	0.4	2
14	Baikal	31,722	23,615	1642	744	201	8.2	330

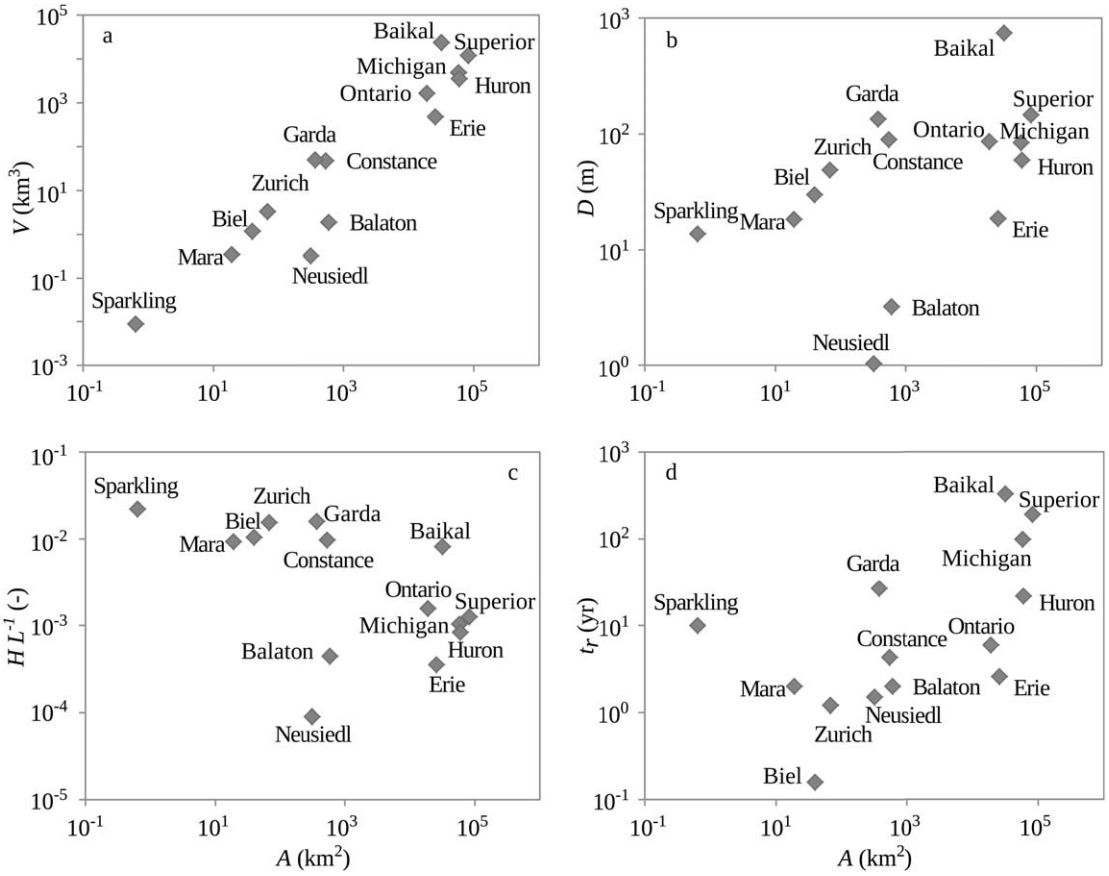

Fig. 2. Variation of the morphological characteristics of the selected lakes as a function of their surface area A (km^2) in a log-log plane: (a) volume V (km^3); (b) mean depth D (m); (c) relative depth HL^{-1} (-); (d) residence time t_r (yr).

Figure 3 shows an example of the application of the model (eight-parameter version) to two lakes characterized by marked differences in the thermal response: Lake Michigan and Lake Neusiedl. Overall, the model is able to reproduce the annual trend satisfactorily, to distinguish between cold and warm seasons (e.g., 1997 vs. 1998 summers in Lake Michigan), and to reproduce correctly short-term fluctuations (e.g., Lake Neusiedl). The major deviations, which can be seen in the case of Lake Michigan during the falling limb of 1995 and in the rising limb of 1996, are likely due to the absence of air temperature measurements (as input of the model) in the two periods, which have been replaced with extrapolated values on the basis of the average year statistics. It is worth noting that, despite this partial lack of data, the model is able to well reproduce the observed lake surface temperatures.

A synthetic information about the air–water temperature behavior can be obtained by considering T_w–T_a diagrams for the mean year (i.e., the data are averaged for each day of the year over the entire data set). Figure 4 shows the hysteresis curves between measured air temperature and both measured and simulated lake surface temperature for some of the examined lakes. The model is able to properly account for the thermal inertia of the water mass and thus to follow the hysteresis between air temperature and lake surface temperature. The qualitative difference between deep lakes (e.g., Lake Superior) and shallow lakes (e.g., Lake Neusiedl) is preserved, as expected, and also well reproduced. In general, the occurrence of the hysteretic behavior depends on the phase lag between the annual variation of air temperature and that of lake surface temperature. The amplitude depends on the thermal inertia of the water volume (the lake surface temperature in larger lakes reacts more slowly to variations of air temperature), whereas the shape (and in particular deviations from elliptic) depends on the variation of the surface layer thickness during the year. Both these aspects will be addressed in the Discussion section.

Some specific features related to the different characteristics of the data sources are, however, worthy of consideration. Lake surface temperatures in Lake Sparkling never go below 1.75°C at 1 m depth, although the lake presumably freezes in winter: in this case, on the basis of the available data, the threshold for ice formation has been assumed as this minimum measured temperature. This produces a hysteresis with a lower limit of T_w that is higher than expected. Satellite data have been considered for Lake Superior because buoy measurements were not available during winter. The lake surface temperature record in Lake Zurich has a monthly frequency, but it is given by occasional measurements, so the dispersion of the points is larger than for other cases. Conversely, monthly values in Lake Balaton are averages, so the trend is smooth. Lake Constance presents a peculiar inversion of the trend of air

Table 2. Available data sets for air and lake surface temperature measurements in the different lakes (only the periods for which the two records are simultaneously available are indicated). Where indicated, B stands for buoy and S for satellite lake surface temperature measurements. In general, air temperature observations are available for longer periods (with respect to lake surface temperature) and typically with subdaily frequency. Particular cases are indicated in the footnotes.

	Period considered in the analysis		Lake surface temperature		Air temperature		
Lake	Period	Length (yr)	Temporal resolution	Sensor depth (m)	Sensor height above ground (m)	Calibration and validation*	Notes
Mara	2001–2012	12	Daily	Surface	6	C	The observation station is located at the lake shore, in correspondence of a connection channel between Lake Shuswap and Lake Mara. The lake level undergoes a mean annual fluctuation of ~ 3 m.
Sparkling	1998–2006	9	Daily	1	2	C	The observation station is installed on a raft equipped with both water-quality instrumentation and meteorological sensors.
Superior (B_1)†	1985–2011	27	Hourly	1	9.8	C+V	The meteorological station (PILM4–Passage Island) is installed on an island, at about 12 m above the lake level.
Superior (B_2)†	1985–2011	27	Hourly	1	35.2	C+V	The meteorological station (STDM4–Stannard Rock) is installed on a lighthouse located at the center of the lake. Buoy series is characterized by missing data during the winter period.
Superior (S)	1994–2011	18	Daily	Satellite		C+V	
Michigan (B)	1985–2011	27	Hourly	0.6	15.5	C+V	The meteorological station (SGNW3–Sheboygan) is installed on a lighthouse located at the lake shore. Buoy series is characterized by missing data during the winter period.
Michigan (S)	1994–2011	18	Daily	Satellite		C+V	
Huron (B)	2004–2012	9	Hourly	0.6	9.1	C	The meteorological station (HRBM4–Harbor Beach) is installed at the lake shore, at about 2 m above the lake level. Buoy series is characterized by missing data during the winter period.
Huron (S)	2004–2012	9	Daily	Satellite		C	
Erie (B)	1985–2011	27	Hourly	0.6	1.5	C+V	The meteorological station (SBIO1–South Bass Island) is installed on an island close to the lake shore, at about 3 m above the lake level. Buoy series is characterized by missing data during the winter period.
Erie (S)	1994–2011	18	Daily	Satellite		C+V	
Ontario (B)	2004–2012	9	Hourly	0.6	NA‡	C	The meteorological station (OSGN6–Oswego) is installed along the lake shore. No information concerning the characteristics of the meteorological station is available. Buoy series is characterized by missing data during the winter period.
Ontario (S)	2004–2012	9	Daily	Satellite		C	
Biel	2000–2013	13.5	Monthly (single measure)	2	2	C	The meteorological station is installed approximately 1.5 km from the lake shore.
Zurich	1981–2012	32	Monthly (single measure)	2	2	C	The meteorological station (Wädenswil) is installed approximately 0.5 km from the lake shore, at about 80 m above the lake level.
Constance	1992–2000, 2004–2007	9+4	20 min or hourly	2.5	2	C+V	Since data are available for two separate periods, the first 9 yr are used for model calibration, whereas the later 4 yr for model validation. The air temperatures at meteorological station (DWD –Konstanz) are measured at about 47 m above lake level.
Garda (B_1)	2009–2012	4	Hourly	10	2	C	The meteorological station is installed at the lake shore. When not available, air temperature data have been integrated with measurements recorded at a meteorological station located about 4 km from the lake.
Garda (B_2)	1990–2011	22	Monthly (single measure)	5		C	The two lake surface temperature series refer to different buoys. The first series (2009–2012) is characterized by several missing data.
Neusiedl	1976–2011	36	Daily	0.8 (average)	2	C+V	The station for lake surface temperature measurement is located on the shoreline. The actual depth of sensor (0.4–1.2 m) depends on water level. The meteorological station (Neusiedl See) is located about 20 m above lake level.

Table 2. Continued.

Lake	Period considered in the analysis		Lake surface temperature		Air temperature	Calibration and validation*	Notes
	Period	Length (yr)	Temporal resolution	Sensor depth (m)	Sensor height above ground (m)		
Balaton	1964–2012	49	Monthly (average)	1–2	2	C+V	Monthly averages are available also for air temperature. In both cases, data are calculated as the average of the values measured at two locations: Siófok (situated 3 m above lake level) and Keszthely (located 12 m above lake level before 1965, 11 m in the period 1966–1995, and 10 m after 1995). Lake monitoring points are located at the shoreline; thus measurements are not necessarily representative of the whole lake.
Baikal	NA‡	NA	Hourly	Variable from 9 to 30 (average 16.9)	2	C	Air temperature is provided from the European Center for Medium-Range Weather Forecasting, and refers to the 40 yr reanalysis data set ERA-40 for the period 1957–2002 with a temporal resolution of 6 h; lake surface temperature is available for 9 yr (2000–2008) for a thermistor chain installed 3.2 km from the northern shore of the South Basin (Piccolroaz and Toffolon 2013). Average years for water and air temperature (calculated over the observation periods) are used in the analysis.

* Notation C + V refers to the cases in which both calibration and validation are performed; C refers only to calibration.
† In this case subscripts 1 and 2 indicate that two different series of air temperature (PILM4 and STDM4) have been used for Lake Superior in the comparison with buoy data.
‡ NA, not available.

temperature during winter, which produces a strange feature in the lower part of the hysteresis cycle. Finally, the mean year in the case of Lake Baikal has been smoothed with a moving average filter to avoid the spurious oscillations due to the short record of lake surface temperature; moreover, a threshold for ice formation higher than 0°C has been considered also in this case because of the relatively large depth of the near-surface sensor (i.e., about 17 m on average; Piccolroaz and Toffolon 2013).

In the ensuing sections we will try first to establish a relation between model parameters and morphological characteristics, and subsequently to discuss the potential use of the model parameters for the interpretation of the main features of the thermal processes characterizing the different lakes.

Defining the surface layer—The model is formulated in such a way that some of the parameters are inversely proportional to the depth of the surface layer, as is suggested for instance by the comparison of Eq. 2 with Eq. 3. In the latter, the temporal variability of the surface volume V_s is included in the volume ratio δ, but the actual value of the reference volume V_r (or the corresponding average depth) is not specified. Moreover, Eq. 2 suggests that a_1, a_2, a_3, and the amplitude of the sinusoidal term a_5 are likely to depend inversely on $D_r = V_r A^{-1}$ However, this dependence is not strict, nor is it possible to establish an a priori estimate of the reference depth. There is no theoretical reason for which V_r should be exactly the whole volume V of the lake: in principle it can be smaller, if only part of the water column reacts to variations of the surface temperature (as can be the case in very deep lakes), or even larger, for instance in those very shallow lakes (e.g., Lake Neusiedl or Lake Balaton) where the thermal inertia of the surface layer may include the effect of a portion of the sediment layer.

To test the capabilities of the model to predict the surface layer thickness we consider here a case study for which long time series of water temperature profiles are available. This is the case of Lake Constance, where temperature profiles have been measured for the years 1992–2000 and 2004–2007. Using these measurements, we estimated the depth of the epilimnion as the smallest depth at which the water density exceeds the density at the surface by 0.2 kg m^{-3}, or alternatively from temperature itself, as the smallest depth at which the water temperature is 1°C lower than that at the lake surface. Then, we calculated the volume of the surface layer extending down to the epilimnion depth using the hypsometric curve of the lake. Dividing the surface volume by the entire volume V of the lake provides an estimate of the volume ratio δ, which changes seasonally (symbols in Fig. 5). The observed δ is limited to values < 0.84 as a consequence of the fact that the deepest available point of the water temperature profile (140.5 m depth) does not coincide with the bottom of the lake (254 m depth). The volume ratio determined from the temperature data is compared with the δ obtained with the eight-parameter and four-parameter versions of the model. Despite the approximations introduced in Eqs. 4

Table 3. Estimated parameters of the eight-parameter model, efficiency index (E), root mean-square error (RMSE), and mean absolute error (MAE) for the calibration and validation periods; when the values are not provided for the latter, the whole record was used for calibration.

	Parameters								Calibration			Validation		
Lake	a_1 (°C d^{-1})	a_2 (d^{-1})	a_3 (d^{-1})	a_4 (°C)	a_5 (°C d^{-1})	a_6 (-)	a_7 (°C)	a_8 (°C)	E	RMSE (°C)	MAE (°C)	E	RMSE (°C)	MAE (°C)
Mara	0.184	0.0189	0.0327	32.97	0.138	0.59	7.71	0.35	0.95	1.70	1.37	—	—	—
Sparkling	0.214	0.0348	0.0466	15.95	0.191	0.538	14.57	0.09	0.99	0.86	0.61	—	—	—
Superior (B_1)	0.00957	0.00472	0.00493	2.84	0.0204	0.315	14.40	0.37	0.90	1.40	1.08	0.88	1.76	1.35
Superior (B_2)	0.00147	0.00618	0.0065	3.08	0.0135	0.262	14.41	0.31	0.90	1.40	1.03	0.89	1.71	1.27
Superior (S)	0.0213	0.00629	0.00879	3.72	0.0229	0.435	14.84	0.49	0.95	1.17	0.88	0.97	1.01	0.69
Michigan (B)	0.026	0.0105	0.0108	6.50	0.0174	0.348	14.08	0.41	0.94	1.67	1.24	0.95	1.57	1.19
Michigan (S)	0.0525	0.00898	0.0128	6.49	0.0369	0.495	11.81	0.41	0.97	1.31	0.97	0.98	1.08	0.78
Huron (B)	0.00616	0.0231	0.0238	9.65	0.0191	0.767	14.72	0.36	0.97	1.27	0.97	—	—	—
Huron (S)	0.0537	0.0144	0.018	7.74	0.0171	0.442	11.64	0.37	0.98	1.06	0.80	—	—	—
Erie (B)	0.0892	0.0627	0.0719	22.45	0.174	0.62	12.74	0.46	0.98	0.93	0.69	0.98	0.94	0.70
Erie (S)	0.13	0.0224	0.0322	10.61	0.104	0.606	12.49	0.47	0.97	1.44	1.05	0.99	0.84	0.64
Ontario (B)	0.00987	0.0217	0.0238	9.84	0.0507	0.63	14.99	0.49	0.94	1.63	1.17	—	—	—
Ontario (S)	0.0611	0.00922	0.0139	9.24	0.0595	0.48	11.99	0.48	0.98	1.11	0.82	—	—	—
Biel	0.187	0.0321	0.0413	11.43	0.079	0.64	4.33	0.09	0.98	0.88	0.68	—	—	—
Zurich	0.113	0.0198	0.0236	7.85	0.0356	0.619	8.74	0.28	0.98	0.90	0.72	—	—	—
Constance	0.157	0.0166	0.0283	5.40	0.0764	0.633	10.82	0.25	0.96	1.18	0.89	0.94	1.34	0.96
Garda (B_1)	0.0265	0.00175	0.00375	10.11	0.0328	0.416	10.01	0.19	0.95	0.94	0.66	—	—	—
Garda (B_2)	0.0452	0.00574	0.00899	9.51	0.0142	0.444	1.53	0.23	0.87	1.81	1.17	—	—	—
Neusiedl	0.881	0.153	0.23	16.17	0.983	0.519	12.27	0.20	0.96	1.61	1.22	0.95	1.72	1.35
Balaton	0.105	0.115	0.124	18.78	0.22	0.505	14.42	0.41	0.99	0.81	0.60	0.98	1.10	0.90
Baikal	0.0251	0.00379	0.00609	3.40	0.0087	0.43	14.75	0.06	1.00	0.17	0.13	—	—	—

and 6, the agreement between measured and simulated δ is fair (Fig. 5), suggesting that the model is able to correctly follow the seasonal variation in the thickness of the surface layer. Notable is the estimation of the degree of summer stratification (small values of δ), which is particularly critical because in this period the thermal response of the lake is much faster (due to the smaller volume affected by the surface heat flux) than during the well-mixed season. The reproduction of the destratification dynamics in autumn (increasing δ) is also satisfactory, whereas a delay

Table 4. Estimated parameters of the four-parameter model, efficiency index (E), root mean-square error (RMSE), and mean absolute error (MAE) for the calibration and validation periods; when the values are not provided for the latter, the whole record was used for calibration.

	Parameters				Calibration			Validation		
Lake	a_1 (°C d^{-1})	a_2 (d^{-1})	a_3 (d^{-1})	a_4 (°C)	E	RMSE (°C)	MAE (°C)	E	RMSE (°C)	MAE (°C)
Mara	0.0344	0.0232	0.0237	34.98	0.95	1.68	1.36	—	—	—
Sparkling	0.159	0.0537	0.0527	17.58	0.99	0.99	0.75	—	—	—
Superior (B_1)	0.0245	0.00529	0.00785	2.30	0.88	1.57	1.10	0.86	1.91	1.39
Superior (B_2)	0.0141	0.00587	0.00810	2.77	0.89	1.50	1.07	0.88	1.77	1.33
Superior (S)	0.0260	0.00963	0.0124	3.53	0.95	1.21	0.91	0.96	1.08	0.79
Michigan (B)	0.0368	0.0116	0.0126	5.75	0.94	1.68	1.24	0.95	1.61	1.22
Michigan (S)	0.0459	0.0148	0.0168	6.39	0.97	1.36	1.03	0.97	1.09	0.82
Huron (B)	0.0106	0.0193	0.0197	9.27	0.97	1.27	0.97	—	—	—
Huron (S)	0.0536	0.0189	0.0224	8.67	0.98	1.03	0.78	—	—	—
Erie (B)	−0.0187	0.0564	0.0541	24.65	0.98	0.94	0.70	0.97	0.99	0.73
Erie (S)	0.0292	0.0291	0.0302	14.25	0.97	1.46	1.03	0.99	0.85	0.61
Ontario (B)	−0.0116	0.0216	0.0207	9.85	0.94	1.65	1.20	—	—	—
Ontario (S)	0.0456	0.0162	0.0184	7.03	0.98	1.19	0.93	—	—	—
Biel	0.0673	0.0236	0.0245	10.18	0.98	0.85	0.64	—	—	—
Zurich	0.0650	0.0226	0.0222	9.46	0.98	0.92	0.72	—	—	—
Constance	0.0435	0.0150	0.0170	6.22	0.95	1.24	0.92	0.93	1.49	1.07
Garda (B_1)	0.0343	0.00605	0.00889	7.92	0.94	0.98	0.72	—	—	—
Garda (B_2)	0.0542	0.00915	0.0129	10.21	0.87	1.79	1.17	—	—	—
Neusiedl	−0.0862	0.182	0.171	16.66	0.94	1.89	1.44	0.94	1.87	1.47
Balaton	−0.131	0.134	0.121	20.20	0.99	0.83	0.62	0.98	1.09	0.87
Baikal	0.0345	0.00470	0.00798	3.72	1.00	0.19	0.15	—	—	—

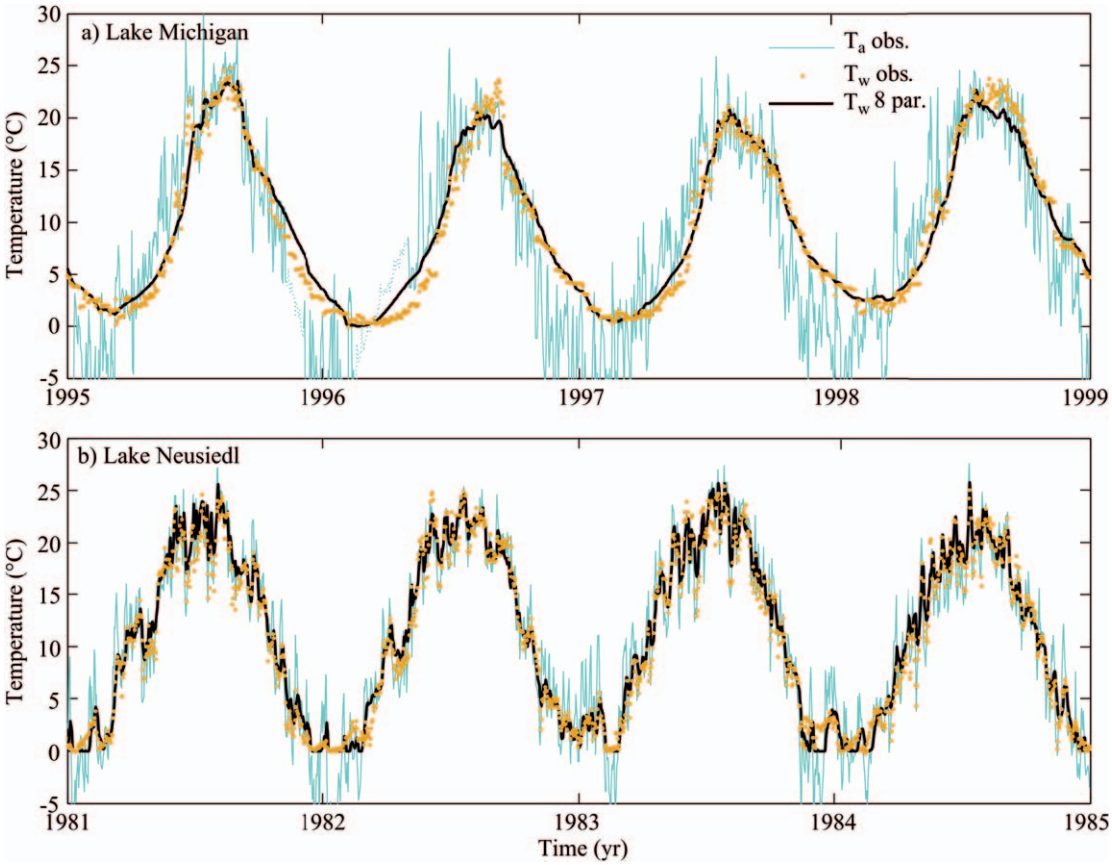

Fig. 3. Time series of air and lake surface temperature for: (a) Lake Michigan; (b) Lake Neusiedl. The observed surface temperature (T_w obs.) has been registered from satellite data (for Lake Michigan) and by a shoreline station (Lake Neusiedl). The modeled surface temperature has been obtained with the eight-parameter model (T_w 8 par.). The observed air temperature (T_a obs.) is also indicated (dotted lines in [a] denote reconstruction of missing periods).

can be noticed in the stratification buildup in spring (decreasing δ), which, however does not jeopardize the overall quality of the results. Notice that the choice of the lake volume V as a scale for making δ dimensionless is arbitrary and may influence the comparison. As a whole, however, the comparison suggests that considering $V_r \cong V$ is reasonable, which corresponds to assuming the average depth as a reference depth ($D_r \cong D$).

Of course, the choice of the average depth may not be appropriate for all cases. For instance, Lake Neusiedl consists of epilimnion only and offers a good example for an intensive heat exchange between air and water. The small water volume has a low heat storage capacity so there are rapid adaptations to short-term weather changes (Fig. 3b). However, the heat exchange between the epilimnion and the soft lake sediment should be considered additionally. Therefore, in this case the effective volume affected by the heat flux can be larger than the mere lake water volume.

Characterization based on model parameters—Aimed at identifying possible scaling features, we analyzed the dependence of the model parameters on all the morphological characteristics of the lakes listed in Table 1. Figures 6 and 7 show a selection of the most relevant dependences for the whole set of parameters. We tested two types of relationships. First, on the basis of the derivation of Eq. 3, some of the parameters (a_1, a_2, a_3, a_5) are expected to depend inversely on depth. This would suggest the use of a power law regression of the type

$$a_i = k_{iX}\ X^{n_{iX}} \tag{7}$$

where i indicates the considered parameter, X is the generic morphological variable (e.g., D, A, t_r, and V) and k_{iX} and n_{iX} suitable regression coefficients. Equation 7 is linear in a double-logarithmic plot and the coefficient R^2 shown in the figures refers to the least-squares regression between the logarithms of a_i and X. The second type of relationship considered in the analysis is a linear function of the logarithm of X:

$$a_i = p_{iX} + q_{iX}\ \ln(X) \tag{8}$$

with p_{iX} and q_{iX} being suitable regression coefficients This relationship accounts for the limited region of existence of some of the parameters (e.g., between 0 and 1 for the phase a_6) as opposed to the variation of the morphological variable X, which changes over several orders of magnitude. In this case the coefficient R^2 refers to the least-squares regression based on Eq. 8. The values of the

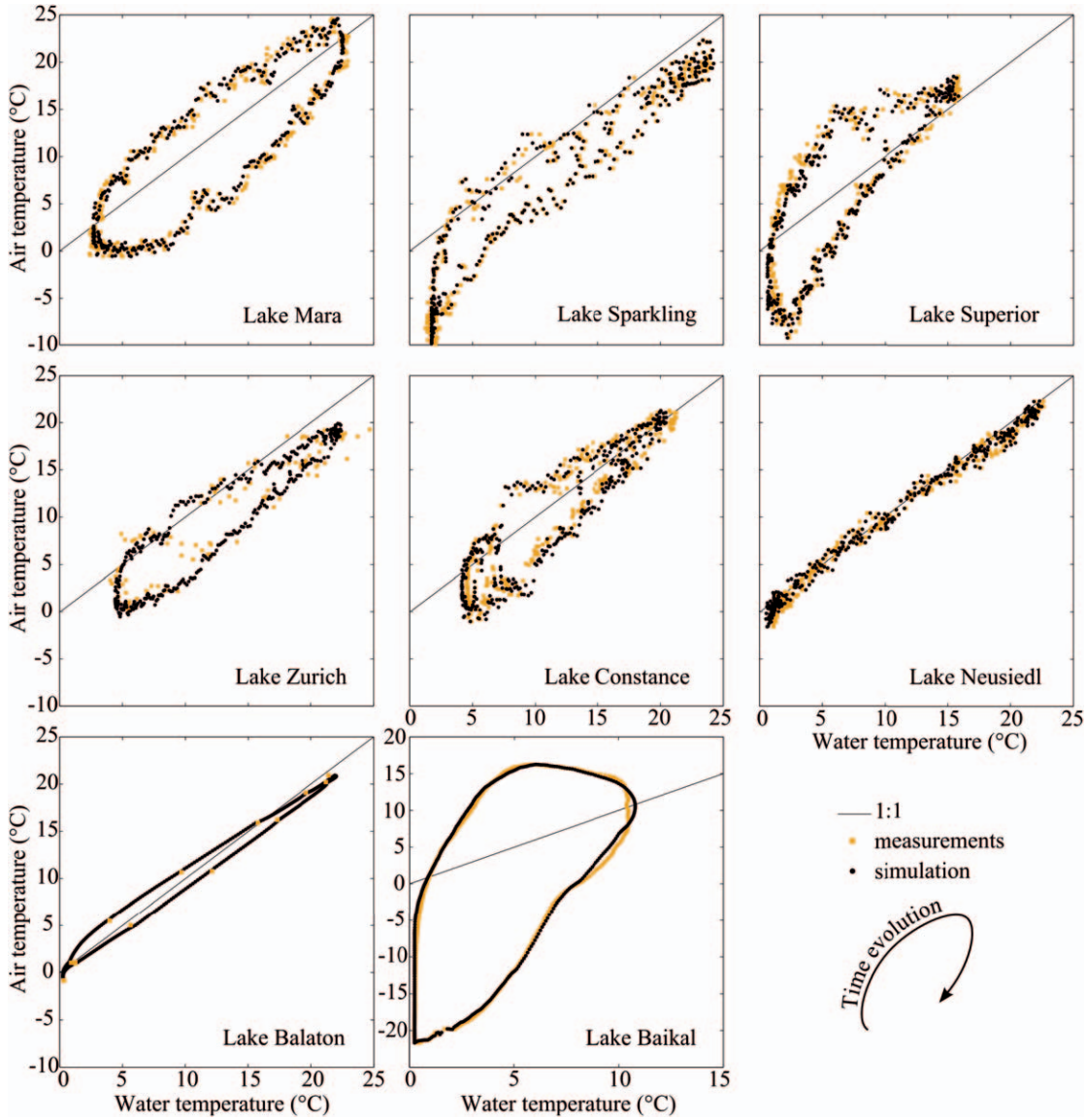

Fig. 4. Hysteresis cycles between air and lake surface temperatures in Lakes Mara, Sparkling, Superior (satellite), Zurich, Constance, Neusiedl, Balaton, and Baikal. Measured and modeled (eight-parameter model) lake surface temperatures are represented with orange squares and black dots, respectively. The range of the axes is the same for all plots with the exception of Lake Baikal.

coefficients n_{iX} and q_{iX} of Eqs. 7 and 8 are summarized in Table 5 together with the value of R^2 used as a measure of the quality of the regression. Notice that the regressions are calculated on 21 members, which include those cases where different sources of information are present (i.e., lake surface temperature from different buoys and from satellite images, air temperature from weather stations located at different heights over the lake) for the same lake (Table 3).

As a preliminary comment, we note that some variability in model parameters exists for the lakes in which different data sources are adopted. This variability is, on the one hand, a positive feature of the model, which can adapt to different sources, but on the other hand may limit the validity of the morphological relationships. However, the mean values of the parameters that have been obtained are consistent with the general trends that are discussed in detail below.

As expected, for some parameters (primarily a_2, a_3, a_5) a significant correlation was found with the average depth D (Table 5). This implies that the lake volume V is a reasonable estimate for the reference volume V_r (i.e., the maximum volume that can be affected by the surface heat flux during complete overturn periods), which is in accordance with the discussion in the previous section. The exponents n_{iX} of the power laws are negative but are not equal to the value -1 that would follow from the structure of Eq. 3. The strongest correlations (highest values of R^2) exist for a_2, a_3, and a_5. The cause for the dependence of the parameters a_2 and a_3 on the mean depth is clear (Fig. 6a,b): these parameters are involved in the thermal response of the lake to variations of air temperature (a_2) and to the resilience of lake surface temperature (a_3), as will be more widely discussed in the next section.

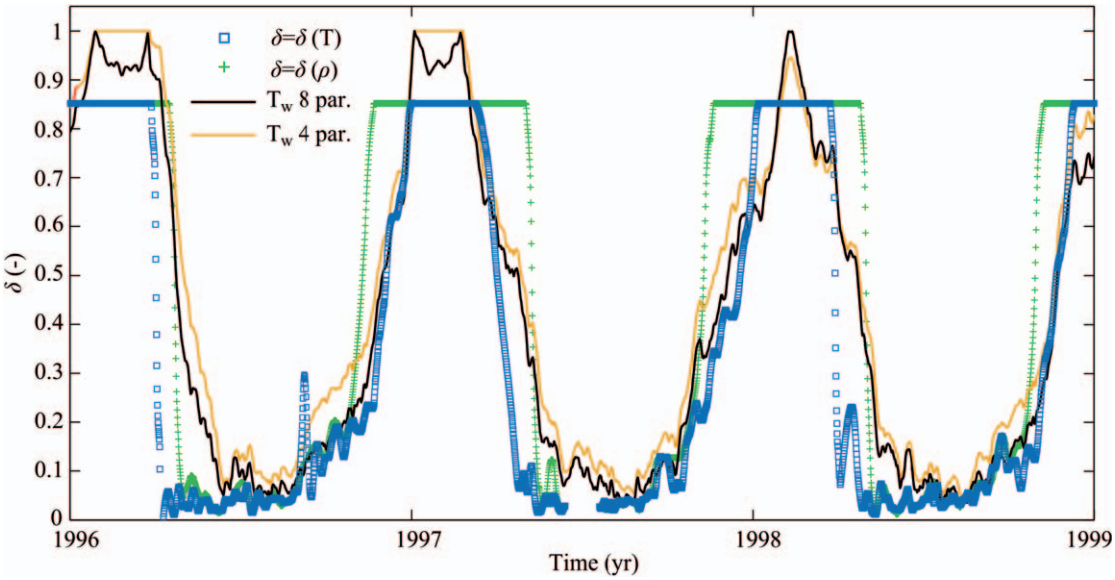

Fig. 5. Seasonal variation of the volume ratio δ: comparison between model results (solid lines) and estimates obtained from measured temperature profiles (symbols) for Lake Constance during 3 yr (1996–1998). Different symbols refer to different methods: squares for estimates based on a threshold directly applied to temperature profiles, crosses based on a threshold on water density.

In the eight-parameter model, the sinusoidal term with amplitude a_5 and phase a_6 sums up all the contributions to the heat budget with the exception of the direct effect of air temperature. Typically, it is primarily associated with the amplitude of the annual variations of the solar radiation. The examined lakes are located approximately at the same latitude; thus the incoming solar heat flux is similar. In this case the value of the amplitude a_5 is highly correlated with the mean depth ($R^2 = 0.83$, Table 6; Fig. 6c), which is the ratio between the volume, i.e., the heat capacity, and the surface through which the flux is transferred. The phase a_6 is distributed around the value 0.5 for almost all lakes. This is consistent with the actual maximum of the solar radiation, which occurs toward the end of June (given the origin of time at 1 January). Interestingly, the strongest correlation in this case is with the residence time t_r (Fig. 6d): higher values of a_6 are noted when the influence of the inflows is stronger (shorter t_r), suggesting that the income of external water tends to postpone the time at which the maximum of the sinusoidal term occurs. Notice that this is consistent with the observation that maximum temperature in rivers occurs much later than the maximum solar radiation.

The parameter a_1, which according to its definition should depend inversely on depth, has been nonetheless analyzed by means of Eq. 8 because it also presents negative values that cannot be included in power law relationships. In this case, different behaviors can be identified for the eight-parameter and four-parameter versions of the model, respectively. In the first case an apparent correlation is observed with the mean depth D, which, however, is primarily due to one single value of a_1 (Lake Neusiedl; if this lake is not included in the regression analysis, the dependence practically disappears). In the second case a correlation is observed with the relative depth HL^{-1} (*see* Table 5), but a weak dependence on D is also present (*see* Fig. 7a).

The parameter a_4 is related to the intensity of the stratification and hence the volume that is affected by the heat exchange. The analysis of the correlations evidences that this parameter is controlled by several factors (t_r, D, and V; Table 5). The dependence on D is shown in Fig. 7b.

The parameters a_7 and a_8 can be defined only for those lakes for which lake surface temperature falls below 4°C and has been measured throughout the whole winter (the latter condition is not frequent because of the common removal of buoys to avoid damage caused by ice). These parameters do not show clear trends with any of the morphological parameters (Table 5), mainly because of the limited number of data that can be used to inform model parameters during the winter periods. Only a mild correlation ($R^2 < 0.3$) can be noted between a_7 and the residence time t_r, and between a_8 and the area A (Fig. 7c,d).

Discussion

Simplified analytical solution—In the previous section we have shown that both the eight-parameter and the four-parameter versions of the model are able to capture the main dynamics of temperature variations in all the lakes considered in the present study (Tables 3, 4). Thus, it is interesting to interpret the role of the different parameters and further investigate their dependence on the morphological characteristics of the lakes. With this aim, we derived an analytical solution for the simpler model, the four-parameter model described by Eq. 5, by introducing some simplifying assumptions. Although the assumptions may be unrealistic, the possibility to obtain an analytical solution allows understanding of the qualitative behavior in

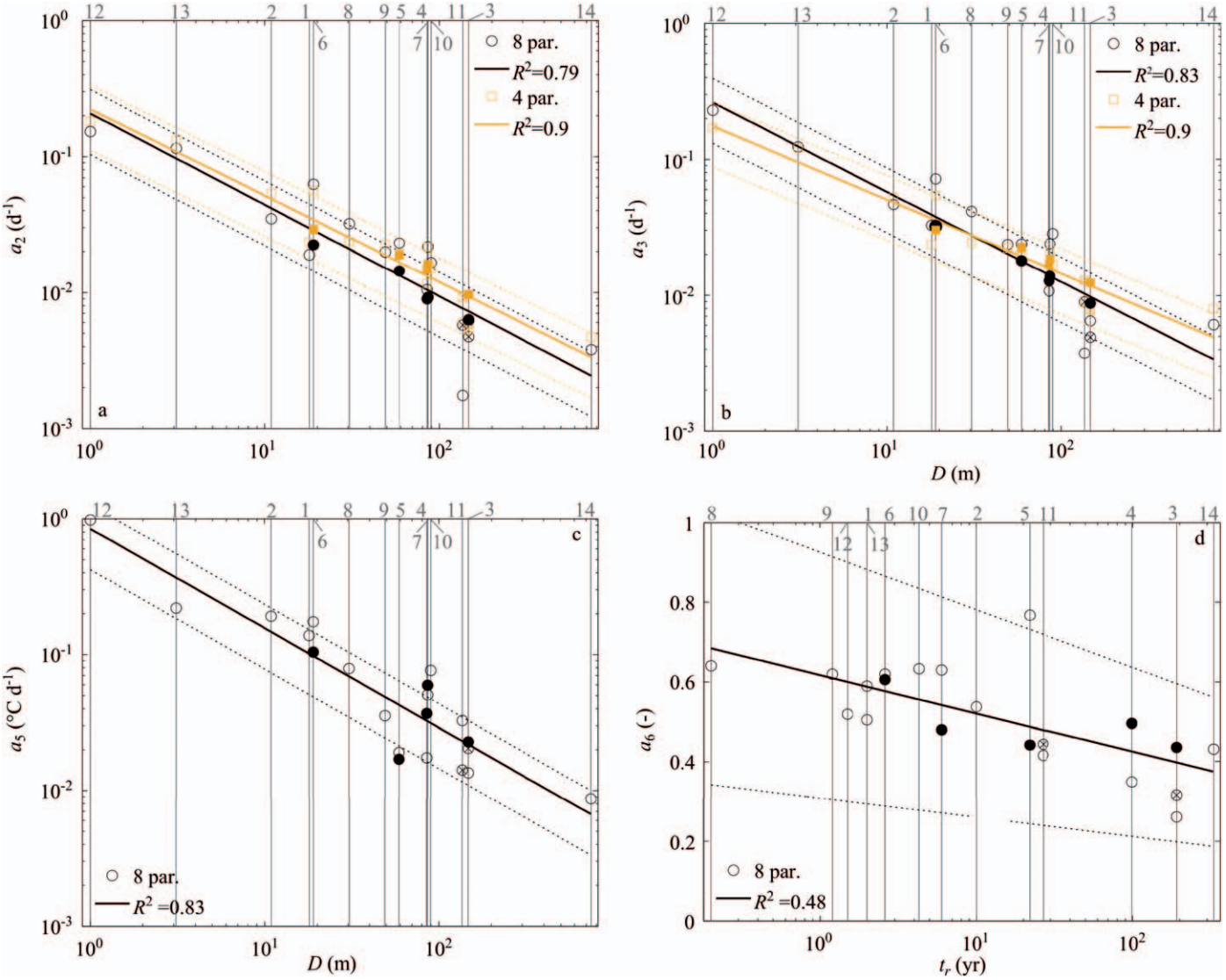

Fig. 6. Relationships between (a) parameter a_2 and mean depth D in a log-log plane; (b) parameter a_3 and mean depth D in a log-log plane; (c) parameter a_5 and mean depth D in a log-log plane; and (d) parameter a_6 and residence time t_r in a semi-log plane. Black circles refer to values obtained from the eight-parameter model, orange squares from the four-parameter model; filling refers to data source: empty for buoy, filled for satellite, internal cross for a different third source that has been considered for a few lakes. Solid lines represent regressions that have been performed with Eq. 7 for a_2, a_3, and a_5, and with Eq. 8 for a_6; R^2 values indicated in the legend are calculated accordingly. Dotted lines indicate deviations of 50% from the solid lines. Numbers at the top refer to the lakes' identification number as in Table 1.

a more evident way. In particular, we assume that the variation of air temperature is sinusoidal, i.e., $T_a = T_{a0} + T_{a1}\sin(\omega t)$, where $\omega = 2\pi/t_y$ is the frequency corresponding to annual variation, T_{a0} is the average temperature over the whole year, T_{a1} is the amplitude of the oscillation, and for sake of convenience the origin of time is set in spring when the air temperature is equal to the average temperature. In addition, we impose a constant value of $\delta = \delta_0$, which means that we consider a fixed value of the average depth of the surface layer. With these assumptions, the parameter a_4 disappears and Eq. 5 can be rewritten in a simplified form,

$$\frac{\mathrm{d}T_\mathrm{w}}{\mathrm{d}t} = \frac{1}{\delta_0}\{a_1 + a_2[T_{a0} + T_{a1}\sin(\omega t)] - a_3 T_\mathrm{w}\}, \qquad (9)$$

which can be solved analytically by imposing the initial condition $T_\mathrm{w}(t = 0) = T_{\mathrm{w}i}$, obtaining the following expression:

$$T_\mathrm{w} = T_{\mathrm{w}i}\exp\left(-\frac{t}{t_\mathrm{d}}\right) + T_{\mathrm{w}0}\left[1 - \exp\left(-\frac{t}{t_\mathrm{d}}\right)\right] + T_{\mathrm{w}1}\left[\sin(\omega t - \phi) + \frac{1}{\sqrt{1 + (\omega t_\mathrm{d})^{-2}}}\exp\left(-\frac{t}{t_\mathrm{d}}\right)\right] \qquad (10)$$

In Eq. 10 the timescale of the adaptation process is

$$t_\mathrm{d} = \frac{\delta_0}{a_3} \qquad (11)$$

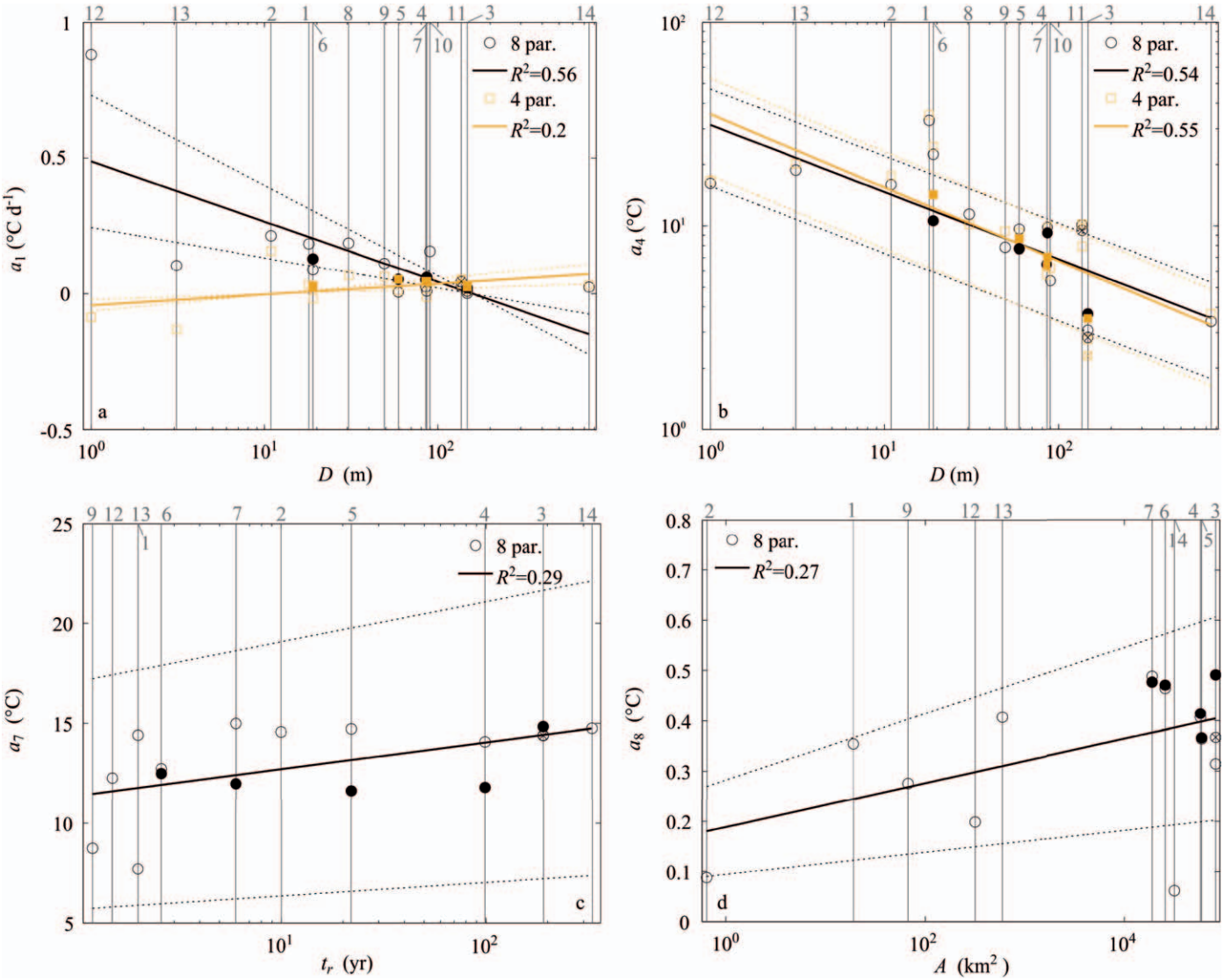

Fig. 7. Relationships between (a) parameter a_1 and mean depth D in a semi-log plane; (b) a_4 and mean depth D in a log-log plane; (c) a_7 and residence time t_r in a semi-log plane; and (d) a_8 and surface area A in a semi-log plane. Notation is the same as in Fig. 6. Regressions are performed with Eq.7 for a_4 and with Eq. 8 for a_1, a_7, and a_8.

and represents the decay time of the initial condition. The annual average lake surface temperature, T_{w0}, is related to T_{a0} through the following linear relationship:

$$T_{w0} = \frac{a_1}{a_3} + \frac{a_2}{a_3} T_{a0} \tag{12}$$

with $a_2\, a_3^{-1}$ being the slope ratio. The amplitude of the sinusoidal oscillation of lake surface temperature, $T_{w1} = \alpha T_{a1}$, is proportional to that of air temperature through the parameter

$$\alpha = \frac{a_2/a_3}{\sqrt{1+(\omega\, t_d)^2}} \tag{13}$$

Eq. 13 suggests that, besides the contribution of $a_2\, a_3^{-1}$, the amplitude T_{w1} is controlled also by the adaptation time t_d, especially when this becomes larger than a few months (e.g., when $\omega t_d = 2\pi t_d/t_y \approx 1$). Finally, the phase lag between the air temperature variations and the lake surface temperature response is

$$\varphi = \arctan(\omega\, t_d) \tag{14}$$

Despite its limitations, Eq. 10 can provide some insight in the process and allows clarification of the role of the different parameters. In particular, exploiting the fact that δ_0 is constant, it is possible to express the oscillations of lake surface temperature after the initial adaptation in a very simple form: for $t >> t_d$ Eq. 10 simplifies into

$$T_w = T_{w0} + T_{w1} \sin(\omega\, t - \varphi) \tag{15}$$

According to Eq. 15, when the phase φ is different from zero a hysteresis develops between air and lake surface temperature, and the breadth of such a hysteresis cycle increases with φ as the adaptation timescale t_d becomes longer.

Table 5. Results of the regression: exponent n_{iX}, defined in Eq. 7, or q_{iX}, defined in Eq. 8, and coefficient R^2 for the parameters (par) a_1 to a_8 and for the other variables defined in the main text, as a function of the morphological properties D, V, t_r, A, HL^{-1}. Best fits are denoted by an asterisk.

			D		V		t_r		A		HL^{-1}	
Parameter	Regression	Version	$n_i\ q_i$	R^2	$n_i\ q_i$	R^2	$n_i\ q_i$	R^2	$n_i\ q_i$	R^2	$n_i\ q_i$	R^2
a_1	Eq. 8	(8-par)	−0.10	0.56*	−0.03	0.35	−0.04	0.22	−0.02	0.18	−0.03	0.10
		(4-par)	0.02	0.20	0.00	0.01	0.00	0.02	0.00	0.08	0.02	0.46*
a_2	Eq. 7	(8-par)	−0.67	0.79*	−0.14	0.32	−0.38	0.51	−0.11	0.11	−0.22	0.13
		(4-par)	−0.64	0.90*	−0.15	0.42	−0.34	0.50	−0.12	0.17	−0.20	0.13
a_3	Eq. 7	(8-par)	−0.66	0.83*	−0.16	0.41	−0.39	0.58	−0.13	0.18	−0.19	0.10
		(4-par)	−0.54	0.90*	−0.12	0.42	−0.27	0.45	−0.10	0.17	−0.19	0.16
a_4	Eq. 7	(8-par)	−0.33	0.54	−0.11	0.50	−0.24	0.55*	−0.11	0.33	−0.01	0.00
		(4-par)	−0.36	0.55	−0.12	0.51	−0.26	0.57*	−0.12	0.34	−0.01	0.00
a_5	Eq. 7	(8-par)	−0.73	0.83*	−0.20	0.53	−0.42	0.53	−0.18	0.28	−0.22	0.11
a_6	Eq. 8	(8-par)	−0.03	0.12	−0.01	0.14	−0.04	0.48*	−0.01	0.10	0.01	0.04
a_7	Eq. 8	(8-par)	0.33	0.06	0.18	0.15	0.58	0.29*	0.25	0.16	−0.37	0.08
a_8	Eq. 8	(8-par)	0.00	0.00	0.01	0.17	−0.01	0.01	0.02	0.27*	−0.03	0.11
$a_1\ a_3^{-1}$	Eq. 8	(8-par)	0.07	0.00	−0.20	0.20	−0.22	0.05	−0.33	0.33	0.56	0.25*
		(4-par)	0.74	0.46*	0.05	0.02	0.34	0.19	−0.05	0.01	0.55	0.37
$a_2\ a_3^{-1}$	Eq. 8	(8-par)	−0.01	0.00	0.01	0.08*	0.01	0.01	0.02	0.15	−0.02	0.08
		(4-par)	−0.08	0.63*	−0.02	0.30	−0.05	0.56	−0.02	0.13	−0.02	0.04
t_d	Eq. 7	(8-par)	0.66	0.83*	0.16	0.41	0.39	0.58	0.13	0.18	0.19	0.10
		(4-par)	0.54	0.90*	0.12	0.42	0.27	0.45	0.10	0.17	0.19	0.16
α	Eq. 8	(8-par)	−0.11	0.49*	−0.02	0.18	−0.07	0.46	−0.01	0.05	−0.02	0.03
		(4-par)	−0.16	0.77*	−0.04	0.41	−0.10	0.61	−0.03	0.18	−0.03	0.05
$\varphi\ (2\pi)^{-1}$	Eq. 7	(8-par)	0.49	0.88*	0.11	0.42	0.26	0.50	0.09	0.18	0.17	0.15
		(4-par)	0.42	0.89*	0.10	0.40	0.19	0.36	0.07	0.15	0.17	0.21

Understanding the role of the parameters—The hysteresis cycle is a suitable descriptor of the lake thermal dynamics and it is therefore interesting to examine how it is affected by the different parameters. For sake of simplicity, we refer to the case of Lake Constance and limit the analysis to the four-parameter model (Eqs. 5 and 6). We consider a variation of the parameters a_1, a_2, a_3, and a_4 of ± 20% with respect to the best values identified in Table 4 and we graphically analyze the modifications of the hysteresis cycle in Fig. 8: (1) an increase (or decrease) of a_1 produces a rigid shift toward higher (or lower) lake surface temperatures; (2) variations of a_2 and a_3 determine similar changes, although in opposite directions, with modifications of both mean lake surface temperature and shape of the hysteresis; and (3) a variation of a_4 produces a deformation of the hysteresis without a significant change of mean lake surface temperature, as one may expect because of its effect on δ only.

As we have observed in Fig. 6, the depth D exerts a strong control on the values of the parameters a_2 and a_3, and ultimately on the hysteresis cycle. In particular, the structure of Eqs. 10 and 11 suggests that a_3 is a good candidate for the synthetic description of the thermal inertia of the lake. Large values of this parameter correspond to small values of t_d and hence to a fast adaptation to the external conditions: this behavior is typical for shallow lakes (Fig. 6b). Estimates of the adaptation time t_d based on Eq. 11 with the assumption that $\delta_0 = 1$ are shown in Fig. 9a: the increasing trend with D is clear, and is dominant with respect to the correlation with the other morphological variables (*see* Table 5). Similarly, the estimate of phase lag φ based on Eq. 14 grows with D (Fig. 9b), suggesting that more time is needed to warm up the water temperature of the surface layer in deep lakes and that these lakes will show wider hysteresis cycles.

The ratio between the increase of T_w and the increase of T_a depends on $a_2\ a_3^{-1}$, as suggested by Eqs. 12 and 13. Shallow lakes are characterized by values of α close to 1 (Fig. 9c), so lake surface temperature closely follows the variation of air temperature. On the contrary, in deep lakes α tends to become smaller, suggesting that strong annual variations of air temperature reflect into more modest oscillation of lake surface temperature (Lakes Superior and Baikal in Fig. 4). However, this is not the only factor involved because the timing of the stratification is important as well. For instance, an anticipated development of the stratification in spring reduces the depth of the surface layer (i.e., δ) and could enhance the warming process during summer, possibly causing exceptionally high lake surface temperatures. This is, for example, the case of Lake Superior in 1998 (Austin and Coleman 2007).

The intensity of the stratification and hence the volume that is affected by the heat exchange is controlled by the parameter a_4. According to Eqs. 4 and 6, for the same difference of temperature between surface (T_w) and deep water (T_h), small values of a_4 tend to produce a stronger reduction of δ with values that become progressively close to 0. This implies that smaller volumes of water contribute to the heat exchange, thus producing higher changes of temperature as a result of the same net heat flux. This is reflected by the shape of the hysteresis curves, which is thinner for lower values of a_4 and broader for larger values (Fig. 8d). The fact that δ varies during the year is a major

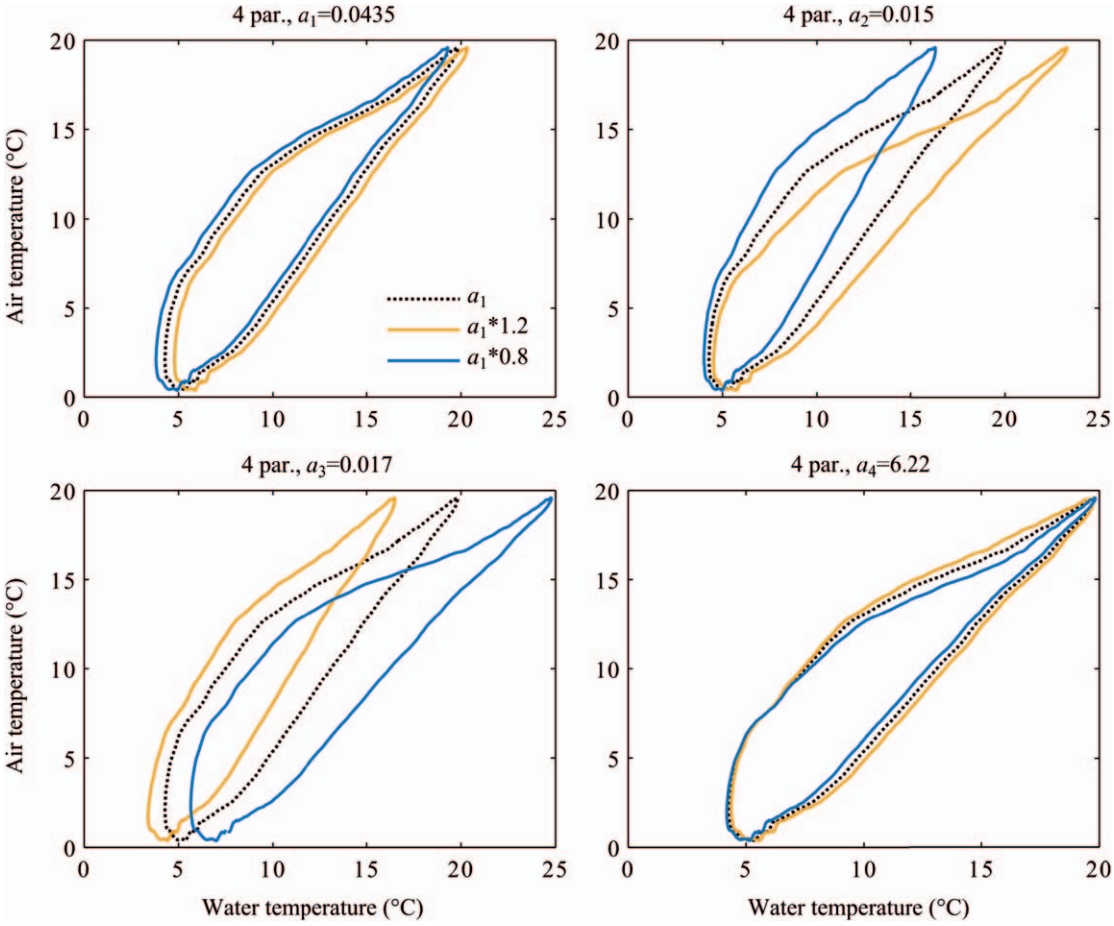

Fig. 8. Effect of a variation of a_1, a_2, a_3, and a_4 on the simulated hysteresis curve for the case of Lake Constance (four-parameter model). With respect to the reference case (dashed line), the hysteresis cycles are modified by increasing and decreasing (± 20%) each of the four parameters reported in Table 4, independently.

difference between the simplified solution (Eq. 10) and the actual behavior. The abrupt variations of δ in the transition from well-mixed to stratified conditions (Fig. 5) determines the fact that the slope of the curve T_w–T_a in the hysteresis loop changes, producing a local bending in some deep lakes (e.g., Lake Superior) characterized by relatively small values of the parameter a_4. Conversely, large values of a_4 determine a milder variation of δ and hence a more regular shape of the hysteresis loop. This is the case for shallow lakes (Fig. 7b), where the water column becomes easily well mixed (this is especially evident in polymictic lakes like Lakes Neusiedl and Balaton) and δ remains not far from 1 throughout the year. Just as an example let us consider a shallow lake (Balaton) and a deeper lake (Constance) with the same maximum difference between T_w and T_h of approximately 15°C. Using the values of a_4 presented in Table 4, Eq. 4 provides an estimate of δ equal to 0.48 for Lake Balaton and 0.09 for Lake Constance. In spite of the large difference in δ values, during the period of maximum stratification the adaptation time $t_d = \delta\, a_3^{-1}$ is similar (between 4 and 5 d) in the two cases, suggesting that the volume affected by the superficial heat budget is comparable, as further confirmed by the similar slope in the upper part (warm season) of the hysteresis curves shown in Fig. 4.

Identifiability of parameters—The selection of the appropriate model formulation requires a robust sensitivity analysis, as typically used in hydrological applications. In particular, we adopted the generalized likelihood uncertainty estimation methodology (Beven and Binley 1992; Majone et al. 2010), which allows for the identification of most important parameters controlling the performance of the model simulation. In our work, the application of the methodology to the various lakes showed that parameter identifiability is better in the four-parameter version than in the eight-parameter version (*see* the case of Lake Superior analyzed in Piccolroaz et al. 2013), although the results of the latter model produce slightly higher Nash–Sutcliffe indices (Tables 3, 4). The problem arises from the possible overparameterization of the mathematical structure of the eight-parameter model presented in Eq. 2, where the forcing terms are essentially three: the term $a_2 T_a$, the term $a_3 T_w$, and the sinusoidal term proportional to a_5. If we assume that $\delta = 1$ and T_a is characterized by an approximately sinusoidal variation along the year, we can obtain an analytical solution for T_w that is sinusoidal and has the same structure as in Eq. 15 but with a more complex formulation for the coefficients T_{w0}, T_{w1}, and φ, which now depend on the five parameters a_1, a_2, a_3, a_5, a_6.

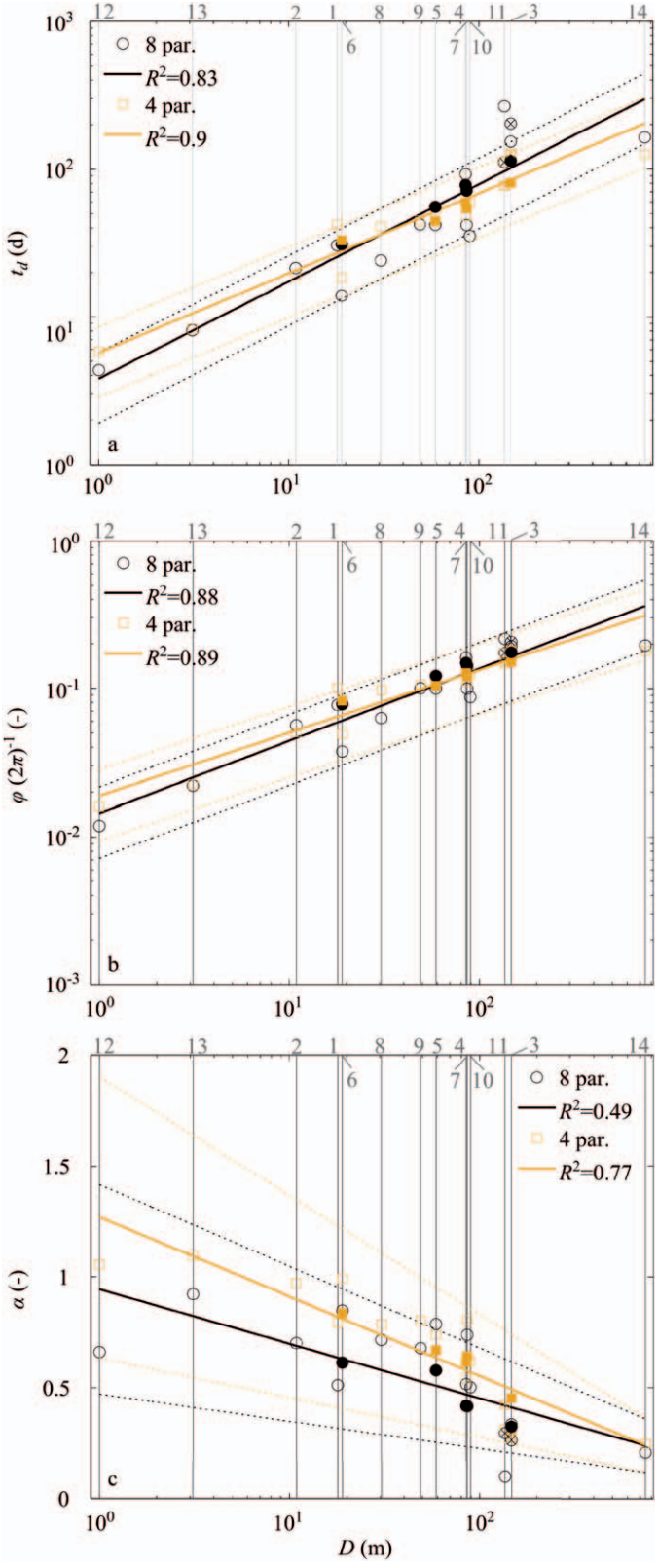

Fig. 9. Estimates of the functions (a) t_d from Eq. 11, (b) φ from Eq. 14, and (c) α from Eq. 13, imposing $\delta_0 = 1$ as a function of the mean depth D. Notation is the same as in Fig. 6, but the regression for α is performed with Eq. 8.

However, if the measurements are approximately sinusoidal, three coefficients are enough to describe the trend, leading to an overparameterization of the problem. On the contrary, this is not the case for the analytical solution (Eq. 15) of the four-parameter model derived under the same assumptions, which is characterized by only three parameters (a_1, a_2, a_3). Of course, the annual variation of T_a and T_w is never exactly sinusoidal in reality, thus justifying the adoption of the eight-parameter model, which requires longer time series and, possibly, a higher degree of interannual variation for a proper calibration.

Accounting for variable δ in the eight-parameter model is in general not a problem for the identifiability of the parameters, except for the cases in which no data are available during winter season, making it impossible to identify a_7 and a_8 in dimictic lakes. Even if these data are available, a_7 and a_8 are not fully independent in the model formulation, which results in a generally poor identifiability. This suggests that a further improvement of the model should focus on a more appropriate parameterization for δ in the case of inverse stratification. The relatively high values derived for a_7 (Table 3), which imply $\delta \sim 1$ for $T_w < 4^\circ$C, support the simplification $\delta = 1$ during inverse stratification.

Further developments—In this paper we have applied air2water, a model to convert air temperature into surface temperatures in lakes, to 14 temperate lakes characterized by different morphological characteristics. The lake surface temperature reconstructed by the model was shown to reproduce the measured values satisfactorily in all the proposed formulations (eight- and four-parameter versions) and also when a limited amount of observed lake temperature data is available. Starting from the more complete data sets with daily values of both air and lake surface temperature, the model has been applied even in those cases where only monthly occasional values were available and for short series (Lake Garda), or considering the mean years for air and lake surface temperature obtained from different periods (Lake Baikal). In particular, the temporally varying relation between air and lake surface temperature, which is due to the thermal inertia of the water mass, was suitably reconstructed both in the case of strong hysteresis and in the case of almost linear relationship.

The parameters of the model are determined through a data-driven calibration that allows for an assimilation of the actual processes occurring in the lake, without the need to look for a detailed description of the various heat fluxes as performed in purely deterministic approaches. In this way we can learn from the values of the parameters, and use them as indicators of the main characteristics of the lake's thermal behavior. The parameters show clear trends suggesting the possibility to define a thermal classification on the basis of lake morphology, where the mean depth plays a major role in determining the lake surface temperature response to varying air temperature signals.

These considerations open new directions: (1) the use of this model to construct regionalization relationships between model parameters and thermal dynamics in

ungauged lakes. For this aim, the model should be applied to several other different lakes, following the approach discussed in this work and possibly including lakes at different latitudes (e.g., tropical and polar lakes). (2) The possibility to estimate the response of different lakes to air temperature variations in climate change effect assessments. In this case, the aim is to provide a simple tool that could be used in contexts where the uncertainty associated with the simplified structure of the model and the determination of the parameters may become negligible with respect to the strong uncertainties present in the future climate projections. (3) The possibility of coupling air2water with atmospheric circulation and weather prediction models. Recent attempts in adopting complex one-dimensional lake models (e.g., using k-ε turbulence model as in Goyette and Perroud 2012) have shown some limitations: expensive computational cost, the need of ground information, and the possible feedbacks between erroneous reproduction of the stratification and unrealistic heating of the surface layer. Simpler models have also been adopted to this aim (dating back to Hostetler et al. 1993), but inevitably require the entire set of meteorological data to infer the heat fluxes on the basis of uncertain empirical relationships. Conversely, the simplicity (i.e., the use of air temperature only) and robustness (i.e., the behavior is controlled by the simple structure of the model) of our formulation makes air2water a good candidate for being adopted as a lumped lake model in meteorological simulations.

Acknowledgments

We are grateful to various people for data provision: Bernhard Kramer (Shuswap Lake Region, Canada, http://www.shuswaplakewatch.com) for Lake Mara; the North Temperate Lakes Long Term Ecological Research Program (http://lter.limnology.wisc.edu), Center for Limnology, University of Wisconsin-Madison for Lake Sparkling; National Oceanic and Atmospheric Administration for the Great Lakes (Superior, Michigan, Huron, Erie, Ontario); the Swiss Federal Office of Meteorology and Climatology of MeteoSwiss for providing air temperature, and Markus Zeh (Amt für Wasser und Abfall, Gewässer- und Bodenschutzlabor, Bern, Switzerland) for lake surface temperature in Lake Biel; Pius Niederhauser (Amt für Abfall, Wasser, Energie und Luft, Zürich, Switzerland) and Oliver Köster (Wasserversorgung der Stadt Zürich, Switzerland) for Lake Zurich; Erich Bäuerle and Dieter Ollinger (Limnological Institute, University of Konstanz, Germany) for lake surface temperature data and the German National Meteorological Service (Deutscher Wetterdienst) for the air temperature data for Lake Constance; Chiara Defrancesco (Agenzia Provinciale per la Protezione dell'Ambiente, Italy) for Lake Garda; Karl Maracek (Hydrographic Service Burgenland, Austria) and Zentralanstalt für Meteorologie und Geodynamik (Austria) for Lake Neusiedl; Kutics Károly (R&D Environmental Consulting and Services llc., Veszprém, Hungary) and Gábor Molnár (Lake Balaton Development Agency, Siófok, Hungary) for Lake Balaton; Michael Sturm (Eawag, Switzerland) and Nikolay M. Budnev (Institute of Applied Physics, Irkutsk State University, Russia) for lake surface temperature, and the European Center for Medium range Weather Forecasting (ECMWF) Data Server (http://data-portal.ecmwf.int) for the ECMWF 40-yr air temperature reanalysis data set from Lake Baikal.

References

Austin, J., and S. Coleman. 2007. Lake Superior summer water temperatures are increasing more rapidly than regional air temperatures: A positive ice–albedo feedback. Geophys. Res. Lett. **34:** L06604, doi:10.1029/2007GL030696

Beven, K. J., and A. M. Binley. 1992. The future of distributed models: Model calibration and uncertainty prediction. Hydrol. Process. **6:** 279–288, doi:10.1002/hyp.3360060305

Boehrer, B., and M. Schultze. 2008. Stratification of lakes. Rev. Geophys. **46:** RG2005, doi:10.1029/2006RG000210

Cho, H.-Y., and K.-H. Lee. 2012. Development of an air–water temperature relationship model to predict climate-induced future water temperature in estuaries. J. Environ. Eng. **138:** 570–577, doi:10.1061/(ASCE)EE.1943-7870.0000499

De Senerpont Domis, L. N., and others. 2013. Plankton dynamics under different climatic conditions in space and time. Freshw. Biol. **58:** 463–482, doi:10.1111/fwb.12053

Eggermont, H., and O. Heiri. 2012. The chironomid–temperature relationship: Expression in nature and palaeoenvironmental implications. Biol. Rev. **87:** 430–456, doi:10.1111/j.1469-185X.2011.00206.x

Goudsmit, G. H., H. Burchard, F. Peeters, and A. Wüest. 2002. Application of k-ε turbulence models to enclosed basins: The role of internal seiches. J. Geophys. Res. **107:** 3230, doi:10.1029/2001JC000954

Goyette, S., and M. Perroud. 2012. Interfacing a one-dimensional lake model with a single-column atmospheric model: Application to the deep Lake Geneva, Switzerland. Water Resour. Res. **48:** W04507, doi:10.1029/2011WR011223

Hostetler, S. W., G. T. Bates, and F. Giorgi. 1993. Interactive coupling of a lake thermal model with a regional climate model. J. Geophys. Res. **98:** 5045–5057, doi:10.1029/92JD02843

Hutchinson, G. E., and H. Löffler. 1956. The thermal classification of lakes. Proc. Natl. Acad. Sci. USA **42:** 84–86, doi:10.1073/pnas.42.2.84

Lewis, W. M. 1983. A revised classification of lakes based on mixing. Can. J. Fish. Aquat. Sci. **40:** 1779–1787, doi:10.1139/f83-207

Livingstone, D. M., and A. F. Lotter. 1998. The relationship between air and water temperatures in lakes of the Swiss Plateau: A case study with palæolimnological implications. J. Paleolimnol. **19:** 181–198, doi:10.1023/A:1007904817619

———, and J. Padisák. 2007. Large-scale coherence in the response of lake surface-water temperatures to synoptic-scale climate forcing during summer. Limnol. Oceanogr. **52:** 896–902, doi:10.4319/lo.2007.52.2.0896

Majone, B., A. Bertagnoli, and A. Bellin. 2010. A non-linear runoff generation model in small Alpine catchments. J. Hydrol. **385:** 300–312, doi:10.1016/j.jhydrol.2010.02.033

Morrill, J. C., R. C. Bales, and M. Conklin. 2005. Estimating stream temperature from air temperature: Implications for future water quality. J. Environ. Eng. **131:** 139–146, doi:10.1061/(ASCE)0733-9372(2005)131:1(139)

Nash, J. E., and J. V. Sutcliffe. 1970. River flow forecasting through conceptual models 1. A discussion of principles. J. Hydrol. **10:** 282–290, doi:10.1016/0022-1694(70)90255-6

Peeters, F., D. M. Livingstone, G. H. Goudsmit, R. Kipfer, and R. Forster. 2002. Modeling 50 years of historical temperature profiles in a large central European lake. Limnol. Oceanogr. **47:** 186–197, doi:10.4319/lo.2002.47.1.0186

Perroud, M., S. Goyette, A. Martynov, M. Beniston, and O. Anneville. 2009. Simulation of multiannual thermal profiles in deep Lake Geneva: A comparison of one-dimensional lake models. Limnol. Oceanogr. **54:** 1574–1594, doi:10.4319/lo.2009.54.5.1574

Piccolroaz, S., and M. Toffolon. 2013. Deep water renewal in Lake Baikal: A model for long-term analyses. J. Geophys. Res. **118:** 6717–6733, doi:10.1002/2013JC009029

———, ———, and B. Majone. 2013. A simple lumped model to convert air temperature into surface water temperature in lakes. Hydrol. Earth Syst. Sci. **17:** 3323–3338, doi:10.5194/hess-17-3323-2013

Sharma, S., S. C. Walker, and D. A. Jackson. 2008. Empirical modelling of lake water-temperature relationships: A comparison of approaches. Freshw. Biol. **53:** 897–911, doi:10.1111/j.1365-2427.2008.01943.x

Stefan, H. G., X. Fang, and M. Hondzo. 1998. Simulated climate change effects on year-round water temperatures in temperate zone lakes. Clim. Chang. **40:** 547–576, doi:10.1023/A:1005371600527

Thiery, W., and others. 2014. LakeMIP Kivu: Evaluating the representation of a large, deep tropical lake by a set of one-dimensional lake models. Tellus A **66:** 1–18, doi:10.3402/tellusa.v66.21390

Wahl, B., and F. Peeters. 2014. Effect of climatic changes on stratification and deep-water renewal in Lake Constance assessed by sensitivity studies with a 3D hydrodynamic model. Limnol. Oceanogr. **59:** 1035–1052, doi:10.4319/lo.2014.59.3.1035

Wetzel, R. G., and G. E. Likens. 1991. Limnological analyses, 2nd ed. Springer-Verlag.

Winder, M., and U. Sommer. 2012. Phytoplankton response to a changing climate. Hydrobiologia **698:** 5–16, doi:10.1007/s10750-012-1149-2

Wojtal-Frankiewicz, A. 2012. The effects of global warming on *Daphnia* spp. population dynamics: A review. Aquat. Ecol. **46:** 37–53, doi:10.1007/s10452-011-9380-x

Associate editor: Roland Psenner

Received: 18 February 2014
Accepted: 26 August 2014
Amended: 03 September 2014